

# Relative cluster entropy for power-law correlated sequences

Anna Carbone  
*Politecnico di Torino Italy*

Linda Ponta  
*LIUC Castellanza Italy*

(Dated: June 7, 2022)

We propose an information-theoretical measure, the *relative cluster entropy* or *clustering divergence*  $\mathcal{D}_C(P||Q)$ , to discriminate among cluster partitions characterised by probability distribution functions  $P$  and  $Q$ . The measure is illustrated with the clusters generated by pairs of fractional Brownian motions with Hurst exponents  $H_1$  and  $H_2$  respectively. For subdiffusive, normal and superdiffusive sequences, the relative entropy sensibly depends on the difference between  $H_1$  and  $H_2$ . By using the *minimum relative cluster entropy* principle, sequences characterized by different correlation degrees are distinguished and optimal Hurst exponent is selected. Then, real-world cluster partitions obtained from US market prices (DJIA, S&P500, NASDAQ) are compared to those obtained from fully uncorrelated sequences (simple Brownian motions) used as model. The *minimum relative cluster entropy* yields optimal Hurst exponents  $H_1 = 0.55$ ,  $H_1 = 0.57$ , and  $H_1 = 0.63$  respectively for DJIA, S&P500, NASDAQ a clear indication of non-markovianity of the sequences. Finally we derive the analytical expression of the *relative cluster entropy* and the outcomes are discussed for arbitrary pairs of probability distribution functions of continuous variables.

## I. INTRODUCTION

Production and exchange of information in complex systems with interacting components can be quantified via entropy measures [1–7]. Discriminating between empirical data and models in terms of information content is interesting from several viewpoints. Consider an experiment with the outcomes obeying the probability distribution  $P$  whereas the distribution  $Q$  is a model for the same experiment. Quantifying the error of the wrong assumption of the model compared to the correct information content is relevant to a broad class of phenomena [8, 9]. Such information-theoretical concepts bring also together the thermodynamic implications intrinsically related to the dynamical evolution of the system under investigation. Hence, the dynamic of the information transferred along subsequent transformative stages of a complex system can be described in terms of divergence of the probability distributions  $P$  at time  $t$  and  $P'$  at a subsequent time  $t'$ .

Entropy concepts and information-theoretical tools are applied in fields as diverse as climate, turbulence, neurology, biology and economics [10–13] and are increasingly adopted in unsupervised learning of unlabelled data where similarity/dissimilarity measures are concerned with dynamic rather than static features of data clustering [14–16]. The *cluster entropy*  $\mathcal{S}_C(P_j)$  is defined as a Shannon entropy measure with  $P_j$  the power-law probability distribution of the clusters formed in a long-range correlated data sets [17, 18].  $\mathcal{S}_C(P_j)$  has proved the ability to quantify heterogeneity and dynamics of long-range

correlated stochastic processes in a broad range of applications [19, 20]. By extending the definition to continuous random variables, the *differential cluster entropy*  $\mathcal{S}_C(P)$  added clues to the meaning of the different contribution of the terms entering the cluster entropy relationship.

In this work, the *relative cluster entropy* or *cluster divergence*  $\mathcal{D}_C(P||Q)$  of the cluster probability distribution  $P$  with respect to a model distribution  $Q$  is proposed. To illustrate how the *relative cluster entropy* operates, synthetic and real-world data featuring power-law distribution behavior are considered. First, the approach is implemented on fractional Brownian motions (*fBms*) with given correlation exponent (Hurst exponent  $H$ ). A systematic dependence of  $\mathcal{D}_C(P||Q)$  on the Hurst exponent is found. The *minimum relative cluster entropy* principle is then implemented as a selection criterion to extract the optimal correlation exponent of the sequence. Furthermore, as a real-world case, we study the divergence  $\mathcal{D}_C(P||Q)$  of financial price series. The probability distribution  $P$  is obtained by ranking the clusters generated in each market price series and compared to the distribution  $Q$  drawn from synthetic data adopted as model. Finally, the *minimum relative entropy* principle yields the best estimate of the correlation exponents of the financial series and quantifies the deviation of the price series from the model.

The manuscript is organized as follows. In Section II the main computational steps of the *relative cluster entropy* method are described for discrete variables. The ap-

proach is illustrated for synthetic data (fractional Brownian motions) and real-world data (market price series). In Section III the *relative cluster entropy* is extended and its expression for continuous variables is derived, conclusions and suggestions for further development are drawn.

## II. METHODS AND RESULTS

In this section, the *relative cluster entropy* approach is described. The interest is towards the development of a divergence measure able to evaluate the situation where a model probability distribution  $Q$  is defined in parallel to the true probability distribution function  $P$  of the cluster partition. The method is applied to stochastic processes obeying power-law distributions like fractional Brownian motion and market prices. Before illustrating how the proposed *cluster divergence* works, a few definitions are recalled.

Consider the time series  $\{x_t\}$  of length  $N$  and moving average  $\{\tilde{x}_{t,n}\}$  of length  $N - n$  with  $n$  the moving average window. For each  $n$ , the function  $\{\tilde{x}_{t,n}\}$  generates a partition  $\{\mathcal{C}\}$  of non-overlapping clusters between consecutive intersections of  $\{x_t\}$  and  $\{\tilde{x}_{t,n}\}$ . Each cluster  $j$  has duration  $\tau_j \equiv \|t_j - t_{j-1}\|$  where the instances  $t_{j-1}$  and  $t_j$  refer to subsequent intersection pairs. The empirical distribution of the frequencies of the cluster duration  $P(\tau_j, n)$  can be obtained by ranking the number of clusters  $\mathcal{N}(\tau_1, n), \mathcal{N}(\tau_2, n), \dots, \mathcal{N}(\tau_j, n)$  according to their duration  $\tau_1, \tau_2, \dots, \tau_j$  for each  $n$  and is defined as:

$$P(\tau_j, n) = \frac{\mathcal{N}(\tau_j, n)}{\mathcal{N}_C(n)} \quad (1)$$

where  $\mathcal{N}_C(n) = \sum_{j=1}^{k(n)} \mathcal{N}(\tau_j, n)$  is the number of clusters generated by the partition for each  $n$ , with  $k = \sum_{n=1}^N \mathcal{N}_C(n)$  the total number of clusters for all possible values of  $n$ .

The cluster entropy  $\mathcal{S}_C[P]$  is obtained by introducing the cluster frequency  $P(\tau_j, n)$  in the Shannon expression:

$$\mathcal{S}_C[P] = \sum_{j,n} P(\tau_j, n) \log P(\tau_j, n) \quad , \quad (2)$$

with the normalization condition:

$$\sum_{n=1}^N \sum_{j=1}^{\mathcal{N}_C(n)} P(\tau_j, n) = 1 \quad . \quad (3)$$

The cluster entropy approach has been applied and provided interesting clues regarding the intrinsic heterogeneity and dynamics of real-world data sequences [19, 20].

Here, the *relative cluster entropy*  $\mathcal{D}_C(P||Q)$  is proposed to quantify the wrong information yield when a model probability distribution  $Q$  is assumed in place of the true probability distribution  $P$ . A measure of distinguishability between two probability distributions  $P$  and  $Q$  is the *Kullback-Leibler divergence*, defined for discrete variables as  $\mathcal{D}_{KL}(P||Q) = \sum_j P_j \log(P_j/Q_j)$ , with the conditions  $\text{supp}(P) \subseteq \text{supp}(Q)$  and  $\mathcal{D}_{KL}(P||Q) \geq 0$ , with  $\mathcal{D}_{KL}(P||Q) = 0$  for  $P = Q$ . The *minimum relative entropy* principle is then adopted as optimization criterion for model selection and statistical inference.

The *relative cluster entropy* is defined in terms of the discrete cluster durations  $\tau_j$  as follows:

$$\mathcal{D}_{j,n}[P||Q] = P(\tau_j, n) \log \frac{P(\tau_j, n)}{Q(\tau_j, n)} \quad , \quad (4)$$

where the index  $j$  refers to the set of clusters with duration  $\tau_j$  occurring in the partition obtained for a given  $n$  and the frequencies  $P(\tau_j, n)$  and  $Q(\tau_j, n)$  satisfy the condition  $\text{supp}(P) \subseteq \text{supp}(Q)$ . By using Eq. (4), the *relative cluster entropy* is written as:

$$\begin{aligned} \mathcal{D}_C[P||Q] &= \sum_{n,j} \mathcal{D}_{n,j}[P(\tau_j, n)||Q(\tau_j, n)] = \\ &= \sum_{n,j} P(\tau_j, n) \log \frac{P(\tau_j, n)}{Q(\tau_j, n)} \quad , \quad (5) \end{aligned}$$

where the index  $n$  runs over the allowed set of time window values,  $n \in (1, N)$ .

To illustrate how the proposed approach operates, pairs of artificially generated fractional Brownian motions (*fBms*) are analysed in terms of the *relative cluster entropy* defined by Eqs. (4-5). *fBms*  $x_t^H$  with  $t \geq 0$  are power-law correlated stochastic processes, defined by a centered Gaussian process with stationary increments and covariance given by  $\langle x_s^H x_t^H \rangle = \frac{1}{2}(t^{2H} + s^{2H} - |t - s|^{2H})$  with  $H \in (0, 1)$  the Hurst exponent. Power-law behaviour of the correlation function implies very slow memory decay and non-Markovianity. Synthetic *fBm* sequences have been generated with assigned Hurst exponent  $H$  and length  $N$  by using the code available at <https://project.inria.fr/fraclab/>. The cluster frequencies  $P(\tau_j, n)$  and  $Q(\tau_j, n)$  have been estimated by counting the number of clusters with duration  $\tau_j$  and window  $n$  for each *fBm*.

Fig. 1 shows the plots of  $\mathcal{D}_j$ , defined by Eq. (4), estimated for cluster frequencies  $P$  obtained from *fBms* with  $H_1$  varying from 0.20 (top-left) to 0.80 (bottom-right). The model  $Q$  has been estimated on clusters obtained from uncorrelated Brownian paths, i.e. *fBms* with  $H_2 = 0.50$ . The values of the Hurst exponents correspond respectively to power-laws cluster correlation exponents  $\alpha_1 = 2 - H_1$  ranging from 1.80 to 1.20, whereas

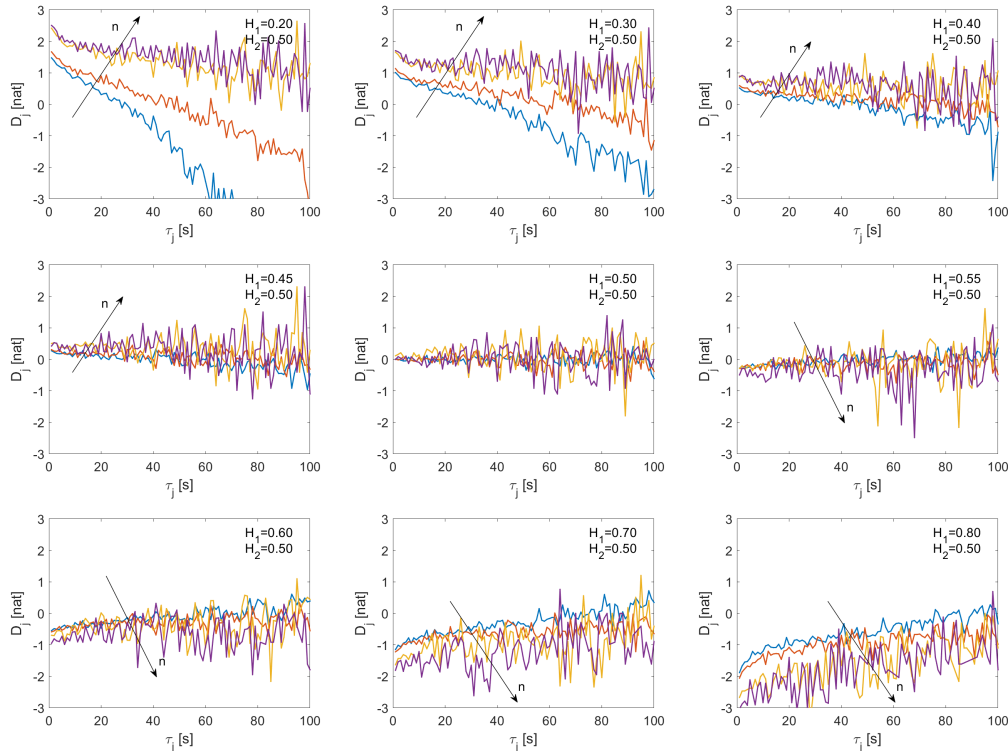


FIG. 1. Plot of  $\mathcal{D}_j$ , defined by Eq. (4), as a function of the cluster duration  $\tau_j$  for  $fBm$  pairs with Hurst exponent  $H_1$  and  $H_2$ . The cluster frequency  $P(\tau_j, n)$  is obtained by counting the occurrences of clusters with duration  $\tau_j$  in fractional Brownian motions with Hurst exponent  $H_1$ . A simple Brownian motion, i.e. a  $fBm$  with  $H_2 = 0.50$ , is taken to obtain the cluster partition and the model probability  $Q(\tau_j, n)$ . In the above figures,  $H_1$  varies respectively from 0.20 (top-left) to 0.80 (bottom-right). The length of the series is equal to  $N = 500000$  for all the graphs. Different curves in each graph refer to different  $n$  values ( $n = 50, 100, 1000, 2000$ ) as indicated by the arrow. At large values of the parameter  $n$ , the curves tend to the asymptotic value  $\mathcal{D}_j = 0$ , expected at large  $\tau_j$ , whereas the curves exhibit a diverging behavior at small values of  $\tau_j$ . At small values of the parameter  $n$  an opposite behaviour is observed, the curves tend to the theoretical value expected at small values of  $\tau_j$ , whereas the curves diverge at large  $\tau_j$ . The properties of the cluster probability divergence  $\mathcal{D}_j$  are discussed in Section III on the basis of the analytical expression of the divergence obtained for continuous variables  $\tau$  (Eq. (10)).

$\alpha_2 = 2 - H_2$  is kept constant and equal to 1.50. In real experiments, small deviations from the model distributions should be reasonably expected. Fig. 1 shows the curves obtained for fractional Brownian motions with  $H_1 = 0.45$ ,  $H_1 = 0.50$  and  $H_1 = 0.55$  with respect to the simple Brownian path, i.e. with respect to a  $fBm$  with  $H_2 = 0.50$  taken as the model in this example. Thus,  $fBm$  pairs with close values of  $H_1$  and  $H_2$  correspond to more realistic experimental conditions. In other words, the situation where Eqs. (4-5) operate on data sequences with correlation exponents close to each other is expected to occur more frequently in the cases of practical interest.

The quantity  $\mathcal{D}_j$  shows characteristic deviations with respect to the null hypothesis (fully random processes with  $H_2 = 0.5$ ). In particular, at small values of the cluster duration  $\tau_j$ , the quantity  $\mathcal{D}_j$  takes positive and negative values respectively for  $fBms$  with  $0.5 < H_1 < 1$  and  $0 < H_1 < 0.5$ . As the cluster duration  $\tau_j$  increases,  $\mathcal{D}_j$

tends to the horizontal axis implying that the divergence between the distributions become negligible for very large clusters.

To further illustrate how the proposed method operates with real-world data, price series  $\{p_t\}$  of Dow Jones Industrial Average (DJIA), Standard and Poor 500 (S&P500), National Association of Securities Dealers Automated Quotations Composite (NASDAQ), are considered. Data includes tick-by-tick prices from January to December 2018. Details (Ticker; Extended name; Country; Currency; Members; Length) as provided by Bloomberg can be found at [www.bloomberg.com/professional](http://www.bloomberg.com/professional). Raw data prices  $\{p_t\}$  have different lengths ( $N_{DJIA} = 5749145$ ,  $N_{S\&P500} = 6142443$ ,  $N_{NASDAQ} = 6982017$ ), thus they are sampled to yield equally spaced data sequences with equal length  $N$  and perform the cluster entropy analysis over comparable data sets.

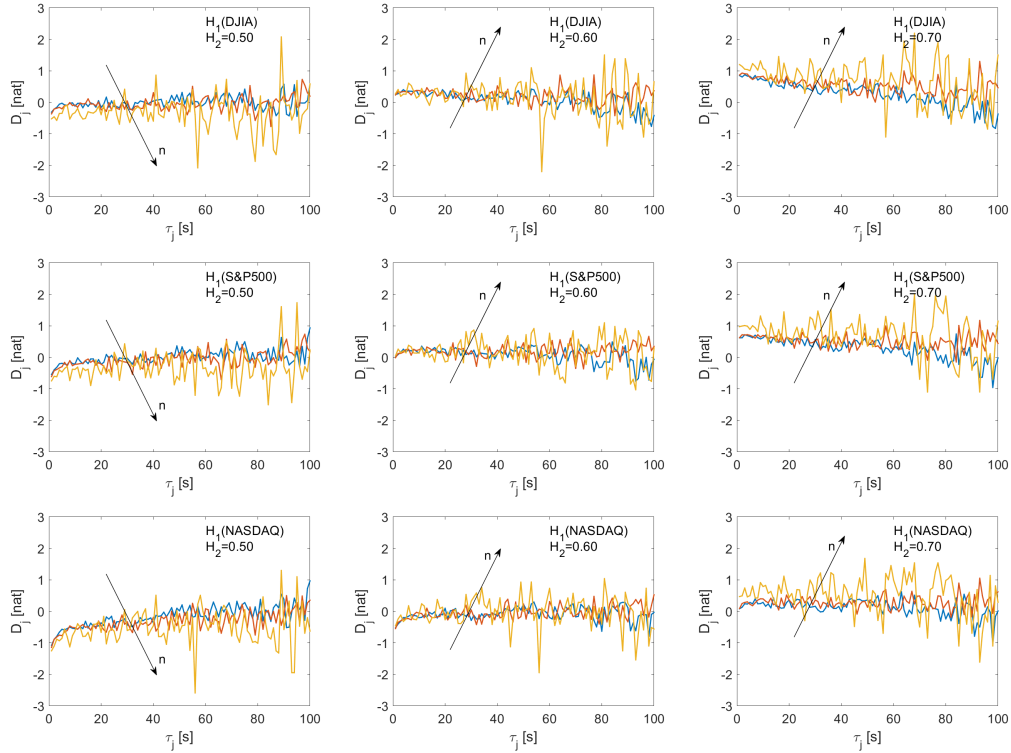


FIG. 2. Plot of the quantity  $\mathcal{D}_j$ , defined by Eq. (4), vs. cluster duration  $\tau_j$ . The cluster frequency  $P(\tau_j, n)$  has been estimated on prices of the DJIA, S&P500, NASDAQ indexes. The model probability  $Q(\tau_j, n)$  has been estimated by considering the cluster generated by a  $fBm$  with Hurst exponent  $H_2$  ranging from 0.50 to 0.70 and length  $N = 492023$  equal to the sampled index series. Different curves in each graph refer to different values of the parameter  $n$  ( $n = 50, 100, 1000$ ).

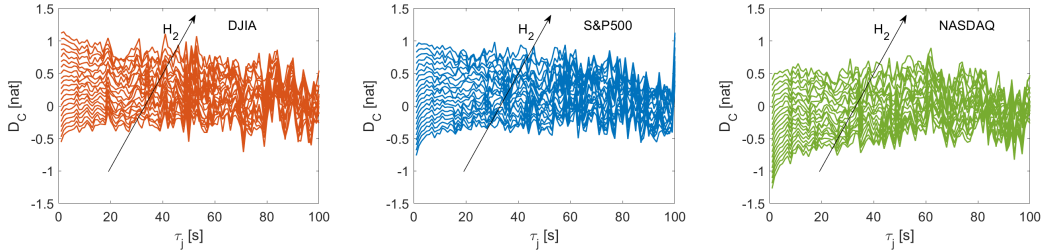


FIG. 3. Plot of the quantity  $\mathcal{D}_C[P||Q]$ , defined by Eq. (5), vs. cluster duration  $\tau_j$ . The curves are obtained by summing the quantities  $\mathcal{D}_j[P||Q]$ , as those shown in Fig. 2, over the parameter  $n$  for the prices of DJIA, S&P500, NASDAQ. Each curve in the figures corresponds to the cluster divergence with the probability  $P(\tau_j, n)$  referred to the market price series  $p_t$  and the model probability  $Q(\tau_j, n)$  referred to  $fBms$  with Hurst exponent  $H_2$  ranging from 0.50 to 0.70 with step 0.1 as indicated by the arrow.

The cluster frequency  $P(\tau_j, n)$  is estimated by counting the clusters generated in the market price series.  $Q(\tau_j, n)$  is estimated by counting the clusters generated in artificially generated stochastic processes assumed as a model of the price series. In the analysis, we consider the divergence between each price series, with unknown correlation exponent and artificially generated samples of fractional Brownian motions  $fBms$  with assigned Hurst exponent  $H_2$ . Results of the analysis are plotted in Fig. 2,

showing the relative cluster entropy for the three markets. Several samples of the curves obtained for different values of the parameter  $n$  shown in Fig. 2 have been summed over the parameter  $n$  with same interval of cluster duration  $\tau_j$ . Fig. 3 shows the relative cluster entropy  $\mathcal{D}_C[P||Q]$  for the data shown in Fig. 2. The *minimum relative entropy* principle is implemented non-parametrically on the values plotted in Fig. 3 by using the relationship:

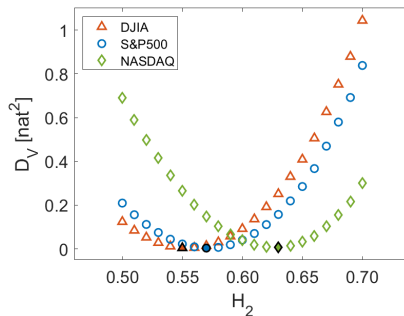


FIG. 4. Plot of the quantity  $\mathcal{D}_V$  defined by Eq. (6) for the relative cluster entropy curves plotted in Fig. 3 vs. the Hurst exponent  $H_2$  of the model distribution  $Q(\tau_j, n)$ . The quantity  $\mathcal{D}_V$  is estimated by means of the variance of  $\mathcal{D}_C$  with respect to 0 (the null hypothesis for  $P = Q$ ) for the market time series in Fig. 3 over the cluster lifetime interval  $1 < \tau_j < 20$ . Each point is evaluated by using the definition given in Eq. (6) for each market and for each  $fBm$  with assigned Hurst exponent  $H_2$ . The Hurst exponent  $H_2$  of the model distribution  $Q(\tau_j, n)$  ranges between 0.50 and 0.70 with step 0.01. The minimum divergence is obtained for  $H_1 = 0.55$  (DJIA),  $H_1 = 0.57$  (S&P500) and  $H_1 = 0.63$  (NASDAQ).

$$\mathcal{D}_V \equiv \frac{1}{k-1} \sum_{j=1}^k [\mathcal{D}_C[P||Q] - \mathcal{D}_C[P=Q]]^2 \equiv \frac{1}{k-1} \sum_{j=1}^k [\mathcal{D}_C[P||Q]]^2 \quad (6)$$

$\mathcal{D}_V$  quantifies the variance of the quantity  $\mathcal{D}_C[P||Q]$ , defined by Eq. (4), around the value  $\mathcal{D}_C[P||Q] = 0$  the null hypothesis expected for  $P = Q$ . The right side of Eq. (6) corresponds to the mean square value of the area of the region between the curves  $\mathcal{D}_C[P||Q]$  and the horizontal axis.  $\mathcal{D}_V$  is a measure of the deviation of the probability distribution of the experimental outcomes with respect to the expected probability distribution function taken as a model. The minimization criterion provided by Eq. (6) has been applied to the data shown in Fig. 3 to yield the best estimate of the correlation degree of the market prices. The value of the Hurst exponent for the series of the prices  $p_t$  has been deduced from the value of  $H_2$  for which  $\mathcal{D}_V$  takes its minimum ( $\mathcal{D}_V = 0$ ) and implies  $H_1 = H_2$ . By using this rule,  $H_1 = H_2 = 0.55$ ,  $H_1 = H_2 = 0.57$ , and  $H_1 = H_2 = 0.63$  are found respectively for the prices of DJIA, S&P500 and NASDAQ. The results of the minimization are shown in Fig. 4 for the markets whose relative cluster entropy is shown in Fig. 3.

### III. DISCUSSION AND CONCLUSION

In this Section, the *relative cluster entropy* will be extended to continuous random variables. For  $N_C(n) \rightarrow \infty$ ,

the characteristic size of generated clusters  $\mathcal{C}$  behaves as continuous random variables  $\tau \in [1, \infty]$  with probability distribution function  $P(\tau)$  varying as a power-law [17, 18]. By taking the limits  $P(\tau_j) \rightarrow P(\tau)d\tau$  and  $Q(\tau_j) \rightarrow Q(\tau)d\tau$ , Eq. (5) can be written for continuous random variables in the form of an integral:

$$\mathcal{D}_C[P(\tau)||Q(\tau)] = \int P(\tau) \log \frac{P(\tau)}{Q(\tau)} d\tau, \quad (7)$$

with  $\tau \in [1, \infty]$ . We are interested in the situations where the probability distributions are power-law functions, i.e. for  $P(\tau)$  and  $Q(\tau)$  respectively in the form:

$$P(\tau) = (\alpha_1 - 1)\tau^{-\alpha_1} \quad Q(\tau) = (\alpha_2 - 1)\tau^{-\alpha_2}, \quad (8)$$

where  $\alpha_1$  and  $\alpha_2$  are the correlation exponents,  $\alpha_1 - 1$  and  $\alpha_2 - 1$  are the normalization constants for  $\tau \in [1, \infty]$ . By using Eqs. (8), Eq. (7) writes:

$$\mathcal{D}_C[P(\tau)||Q(\tau)] = \int (\alpha_1 - 1)\tau^{-\alpha_1} \log \frac{(\alpha_1 - 1)\tau^{-\alpha_1}}{(\alpha_2 - 1)\tau^{-\alpha_2}} d\tau, \quad (9)$$

that after integration becomes:

$$\mathcal{D}_C[P(\tau)||Q(\tau)] = \tau^{1-\alpha_1} \left\{ \log \left( \frac{\alpha_1 - 1}{\alpha_2 - 1} \right) + \left[ \log \tau^{(\alpha_1 - \alpha_2)} + \frac{(\alpha_1 - \alpha_2)}{1 - \alpha_1} \right] \right\} + C, \quad (10)$$

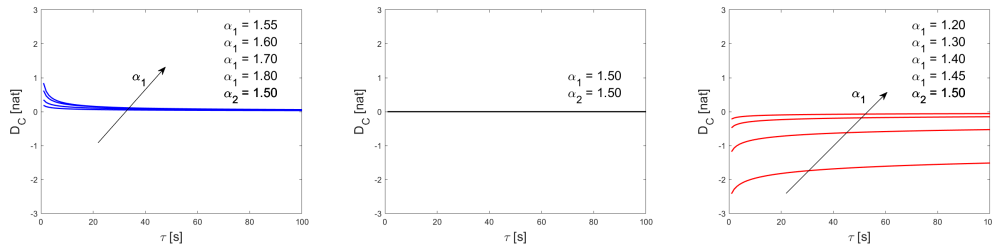


FIG. 5. Plot of the quantity  $\mathcal{D}_C[P||Q]$ , defined by Eq. (10), vs. the cluster duration  $\tau$ . Blue curves (left panel) correspond to a power law probability distribution  $P(\tau)$  with  $\alpha_1$  ranging between  $1.55 \div 1.80$ . The model probability distribution  $Q(\tau)$  is a power law with correlation exponent  $\alpha_2 = 1.50$ , the same for all the curves plotted here. Red curves (right panel) correspond to a power law probability distribution with  $\alpha_1$  ranging between  $1.20 \div 1.45$ . The black line (middle panel) corresponds to the null hypothesis  $\mathcal{D}_C[P||P] = 0$  obtained with  $\alpha_1 = 1.50$  and  $\alpha_2 = 1.50$ .

where the integration constant  $C$  is obtained by setting the condition  $\mathcal{D}_C[P||P] = 0$  which yields  $C = 0$ . By estimating Eq. (10) over the interval  $[1, \infty]$ , the definite integral yields:

$$\mathcal{D}_C[P||Q] = \log\left(\frac{\alpha_1 - 1}{\alpha_2 - 1}\right) - \left(\frac{\alpha_1 - \alpha_2}{\alpha_1 - 1}\right), \quad (11)$$

that for  $\alpha_1 = \alpha_2$ , i.e. for the distribution  $P$  coincident with the model distribution  $Q$ , provides  $\mathcal{D}_C[P||Q] = 0$ .

$\mathcal{D}_C[P||Q]$  quantifies the divergence between  $P(\tau)$  and  $Q(\tau)$ , respectively true and model distribution, as a function of the cluster lifetime  $\tau$  in terms of the different correlation exponents  $\alpha_1$  and  $\alpha_2$ . In Fig. 5, Eq. (10) is plotted as a function of  $\tau$  for different values of the exponents  $\alpha_1$  and  $\alpha_2$ . At small values of the cluster duration ( $\tau \rightarrow 1$ ),  $\mathcal{D}_C[P||Q]$  is strongly dependent on the difference of the power-law exponent  $\alpha_1$  with respect to the exponent  $\alpha_2$  of the model distribution. Conversely, as the cluster duration increases ( $\tau \gg 1$ ),  $\mathcal{D}_C[P||Q]$  tends to become negligible. The decay can be understood by considering that as  $\tau$  increases the cluster becomes disordered as a consequence of the spread of the distribution and the onset of finite-size effect and so the correlation vanishes as the process becomes almost fully uncorrelated. The behaviour of the cluster distribution divergence obtained by using continuous variables is consistent with the empirical tests performed on discrete data sets. In particular, the behaviour shown by fractional Brownian motions with different correlation exponents discussed in the Section II is reproduced by the curves shown in Fig. 5, confirming that the approach is sound.

The *relative cluster entropy* can be therefore exploited to

estimate the deviation of the power law exponent corresponding respectively to true and model probability distributions.

Long-range correlated processes obeying power-law distributions occur frequently in complex system data related to several natural and man-made phenomena. Due to their ubiquity, the extent of long-range correlation and the scaling exponents are relevant to many disciplines, though several difficulties are met for their estimation which require suitable computational procedures to be carefully implemented [21]. A random variable  $x$  obeys a power law if it is drawn from a probability distribution  $p(x) \propto x^{-\alpha}$  with the parameter  $\alpha > 1$  the correlation exponent (scaling exponent). Empirical real-world data barely follow a power-law for all the values of  $x$ . Due to normalization requirements and finite-size effects, ideal power-law behaviour usually holds at values greater than some minimum  $x_{\min}$  up to a maximum  $x_{\max}$ . An exponential cut-off is often artificially introduced to account for the deviation from the ideal power-law behaviour  $x^{-\alpha}e^{-\lambda x}$ . The proposed *relative cluster entropy* approach yields the optimal value of the correlation exponent  $\alpha$  without relying on the estimate of the slope in a log-log plot and thus is robust against computational biases.

The non-parametric minimization of the relative entropy has some advantages compared to parametric approaches, whose implementation requires normality of the random variables and knowledge of the first two moments of the distribution for the calculation of the Lagrange multipliers.

[1] Carlo Cafaro, Sean Alan Ali, and Adom Giffin. Thermodynamic aspects of information transfer in complex dy-

namical systems. *Physical Review E*, 93(2):022114, 2016.

- [2] Juan MR Parrondo, Jordan M Horowitz, and Takahiro Sagawa. Thermodynamics of information. *Nature physics*, 11(2):131–139, 2015.
- [3] Ryoichi Kawai, Juan MR Parrondo, and Christian Van den Broeck. Dissipation: The phase-space perspective. *Physical review letters*, 98(8):080602, 2007.
- [4] Jordan M Horowitz and Massimiliano Esposito. Thermodynamics with continuous information flow. *Physical Review X*, 4(3):031015, 2014.
- [5] Susanne Still, David A Sivak, Anthony J Bell, and Gavin E Crooks. Thermodynamics of prediction. *Physical review letters*, 109(12):120604, 2012.
- [6] Pedro A. Ortega and Daniel A. Braun. Thermodynamics as a theory of decision-making with information-processing costs. *Proceedings of the Royal Society A: Mathematical, Physical and Engineering Sciences*, 469(2153):20120683, 2013.
- [7] X San Liang and Richard Kleeman. Information transfer between dynamical system components. *Physical review letters*, 95(24):244101, 2005.
- [8] Junya Chen, Jianfeng Feng, and Wenlian Lu. A wiener causality defined by divergence. *Neural Processing Letters*, 53(3):1773–1794, 2021.
- [9] Vlatko Vedral. The role of relative entropy in quantum information theory. *Reviews of Modern Physics*, 74(1):197, 2002.
- [10] Richard Kleeman. Measuring dynamical prediction utility using relative entropy. *Journal of the atmospheric sciences*, 59(13):2057–2072, 2002.
- [11] Carlos Granero-Belinchón, Stéphane G Roux, and Nicolas B Garnier. Kullback-leibler divergence measure of intermittency: Application to turbulence. *Physical Review E*, 97(1):013107, 2018.
- [12] David Backus, Mikhail Chernov, and Stanley Zin. Sources of entropy in representative agent models. *The Journal of Finance*, 69(1):51–99, 2014.
- [13] Arturo Tozzi and James F Peters. Information-devoid routes for scale-free neurodynamics. *Synthese*, 199(1):2491–2504, 2021.
- [14] Theresa Ullmann, Christian Hennig, and Anne-Laure Boulesteix. Validation of cluster analysis results on validation data: A systematic framework. *Wiley Interdisciplinary Reviews: Data Mining and Knowledge Discovery*, page e1444, 2021.
- [15] Marina Meilă. Comparing clusterings—an information based distance. *Journal of multivariate analysis*, 98(5):873–895, 2007.
- [16] T Warren Liao. Clustering of time series data—a survey. *Pattern recognition*, 38(11):1857–1874, 2005.
- [17] A. Carbone, G. Castelli, and H. E. Stanley. Analysis of clusters formed by the moving average of a long-range correlated time series. *Physical Review E*, 69:026105, Feb 2004.
- [18] A. Carbone and H. E. Stanley. Scaling properties and entropy of long-range correlated time series. *Physica A: Statistical Mechanics and its Applications*, 384(1):21–24, 2007.
- [19] A. Carbone. Information measure for long-range correlated sequences: the case of the 24 human chromosomes. *Scientific Reports*, 3:2721, 2013.
- [20] Linda Ponta, Pietro Murialdo, and Anna Carbone. Information measure for long-range correlated time series: Quantifying horizon dependence in financial markets. *Physica A: Statistical Mechanics and its Applications*, page 125777, 2021.
- [21] Aaron Clauset, Cosma Rohilla Shalizi, and Mark EJ Newman. Power-law distributions in empirical data. *SIAM review*, 51(4):661–703, 2009.